Journal of Alloys and Compounds, 194 (1993) 389–400
JALCOM 7202

In situ studies of amorphization of the Ge–Al and Si–Al systems induced by 1 MeV electron irradiation

X. W. Lin* and D. N. Seidman**
Northwestern University, Department of Materials Science and Engineering and the Materials Research Center, Robert R. McCormick School of Engineering and Applied Science, 2225 Sheridan Road, Evanston, IL 60208-3108 (USA)

P. R. Okamoto
Argonne National Laboratory, Materials Science Division, Building 212, Argonne, IL 60439 (USA)

(Received December 9, 1991; in final form March 13, 1992)

Abstract

Ge–Al and Si–Al bilayer specimens, and also Al–2.3at.%Ge two-phase alloy specimens, were irradiated *in situ* with 1 MeV electrons at temperatures in the range 10–190 K in a high voltage electron microscope. The Ge precipitates in the Al–2.3at.%Ge alloy disappeared completely at a critical fluence (Φ_c) of approximately 2.4×10^{23} cm^{-2} (24 displacements per atom (dpa) in Ge and 14 dpa in Al) for specimens irradiated at 10 or 50 K; this is the same value of Φ_c at which Ge–Al bilayers are found to contain an amorphous phase. At 10 K an irradiated Ge–Al bilayer specimen is found to have an amorphous phase at the interface only when a Ge layer faces the incident electron beam, while for a Si–Al bilayer specimen amorphization occurs at the interface independent of the direction of the incident beam with respect to a bilayer. For Ge–Al bilayer specimens Φ_c is approximately 2.5×10^{23} cm^{-2} (25 dpa in Ge and 15 dpa in Al). For Si–Al bilayers Φ_c is approximately 3×10^{23} cm^{-2} (19 dpa in Si and 18 dpa in Al). The temperature dependence of Φ_c is also studied for a Ge–Al bilayer specimen. The value of Φ_c is a constant for $T < \approx 160$ K, and then it increases rapidly with increasing T; Φ_c becomes immeasurably large (more than 70 dpa in Ge and more than 43 dpa in Al) at a critical temperature of about 190 K. The temperature dependence of the crystalline to amorphous transition is explained in terms of a recoil-implantation mechanism, coupled with a radiation-enhanced monovacancy diffusion mechanism for Ge atoms in Al, and an athermal contribution to Ge diffusion in Al via an electron-beam stimulated monovacancy migration mechanism.

1. Introduction

Formation of an amorphous phase at the interface region between Si or Ge and a pure metal (*e.g.* Au and Pd) can be observed during a high-energy electron-beam irradiation experiment [1]. This phenomenon is of interest because electron irradiation experiments do not render elemental crystalline Si or Ge specimens amorphous at temperatures as low as 10 K [2–5], while Si or Ge specimens are readily amorphized when ion irradiated at room temperature (T) to a fluence of less than 1 displacement per atom (dpa); *e.g.* see refs. 6 and 7. Two-phase Al–0.7at.%Ge or Al–0.94at.%Ge alloy specimens containing plate-shaped Ge precipitates were claimed to undergo a crystalline to amorphous (c-to-a) transition when irradiated with 1 or 2 MeV electrons at 143 or 170 K [8, 9]. Two mechanisms have been proposed to account for this result. First, the c-to-a transition is attributed to the amorphization of Ge precipitates when the vacancy concentration in the Ge precipitates exceeds a critical value [8]. The Ge–Al interface is assumed to act as a biased sink for mobile Ge self-interstitial atoms (SIAs) generated during electron irradiation; this is suggested to lead to a steady-state vacancy concentration significantly greater than the vacancy supersaturation in an electron-irradiated pure Ge specimen. A second set of experiments, however, suggests a different mechanism [9]. In fact, the latter researchers observed that amorphization occurs initially at the interface farthest from the incident electron beam, when the normal to a plate-shaped Ge precipitate is parallel to the direction of the incident beam [9]. Amorphization should therefore result from the formation of an alloy at a Ge–Al interface via an irradiation-induced recoil-implantation mechanism. The recoiling of Ge atoms into an Al matrix as a result of the elastic transfer of energy from the high-energy electron beam plays an essential role in this mechanism,

*Present address: Lawrence Berkeley Laboratory, 1 Cyclotron Road, Berkeley, CA 94720, USA.
**Also at Argonne National Laboratory, Materials Science Division, Building 212, Argonne, IL 60439, USA.

0925-8388/93/$6.00

and it is different from the mechanism suggested in ref. 8.

To understand in detail the mechanism of the amorphization process occurring at Ge–Al or Si–Al interfaces during an electron irradiation, we performed *in situ* 1 MeV electron irradiation studies on Ge–Al and Si–Al bilayer specimens at temperatures in the range 10–190 K in the 1 MeV high voltage electron microscope (HVEM) at the Argonne National Laboratory. The specimens were prepared by vapor deposition of an Al layer onto a prethinned Ge or Si disk. For an irradiation at 10 K it was found that for Ge–Al bilayer specimens amorphization occurs only when the Ge side of a bilayer specimen faces the incident beam, while for Si–Al specimens amorphization occurs independently of the direction of the incident beam. Critical irradiation fluences (Φ_c's) for a c-to-a transition to occur were measured. We also studied the temperature dependence of Φ_c for amorphization of a Ge–Al bilayer specimen, and found that a critical temperature (190 K) exists above which *no* amorphization is observed. In addition, Al–2.3at.%Ge two-phase alloy specimens containing Ge precipitates were irradiated at 10 or 50 K with 1 MeV electrons. The Ge precipitates disappeared completely at $\Phi_c \approx 24$ dpa for Ge, and this is the same value of Φ_c at which Ge–Al bilayers are found to contain an amorphous phase at the Ge–Al interface. The temperature dependence of the c-to-a transition for Ge–Al bilayers is explained in terms of a recoil-implantation mechanism, coupled with a radiation-enhanced monovacancy diffusion mechanism for the Ge atoms in Al, and an athermal contribution to Ge diffusion in Al via an electron-beam stimulated monovacancy migration mechanism [10, 11].

2. Experimental procedures

We prepared: (i) Al–2.3at.%Ge alloy specimens containing pure Ge precipitates in an Al matrix; (ii) Ge–Al and Si–Al bilayer specimens.

(i) Specimens with pure Ge precipitates were obtained in an Al–2.3at.%Ge alloy, in the form of a foil, which had been heat-treated by a combined quenching and aging procedure, *i.e.* a foil was solution-treated at 770 K and then quenched into an iced-brine solution; it was then annealed immediately at 430 K for 10 h to grow the Ge precipitates. After this heat treatment HVEM specimens were prepared by electrolytically jet-polishing disks with a diameter of 3 mm employing a solution of 20% perchloric acid and 80% ethyl alcohol; the disks were cut directly from the foils. We observed the specimens initially by conventional transmission electron microscopy (TEM). Figure 1 is a bright-field micrograph of a specimen showing plate-shaped Ge precipitates in an Al matrix; the inset is the corresponding selected area diffraction pattern (SADP). The Ge precipitates are single crystals and their orientation relationship with the Al matrix is $[110]_{Al}//[110]_{Ge}$ and $\{111\}_{Al}//\{111\}_{Ge}$; this relationship is consistent with other results [12, 13].

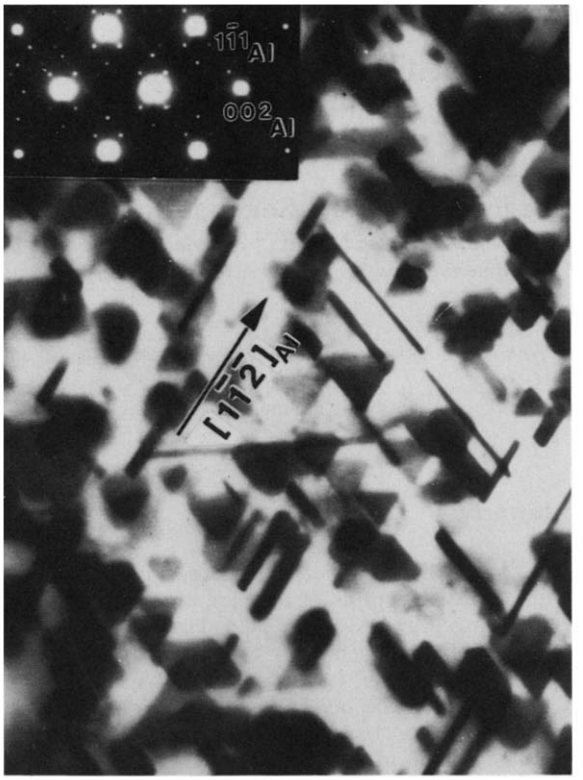

Fig. 1. A TEM image exhibiting Ge precipitates in an Al–2.3at.%Ge alloy specimen after a combined quenching and aging heat treatment. The inset is the corresponding SADP with a [110] zone axis. The strong spots correspond to reflections from the Al matrix and the weak ones, surrounding the Al reflections, from Ge precipitates.

(ii) Ge–Al or Si–Al bilayer specimens were prepared by vapor deposition of Al onto Ge or Si disks with a diameter of 3 mm that were cut from Ge wafers with a [110] normal or Si wafers with a [111] normal. The Ge or Si disks were thinned by grinding, followed by dimpling, and finally chemical etching with a solution of $HF:H_2O_2:H_2O$ (2:1:30 by volume) for Ge disks and a solution of $HF:HNO_3$ (1:9 by volume) for Si disks. The thinned disks were rinsed in deionized water before they were inserted into a vacuum evaporator. An Al layer 40 nm thick was vapor-deposited onto the Ge or Si disks at room temperature at a pressure of approximately 10^{-6} Torr; the deposition rate was 1 nm s^{-1}. The vapor-deposited Al layers were polycrystalline with a grain diameter of about 100 nm.

In situ 1 MeV electron irradiation experiments were performed in a 1 MeV HVEM equipped with a specially fabricated liquid-helium cooled double-tilt stage [14]. This stage allowed us to maintain a specimen at any

temperature between about 10 and 300 K during an irradiation. For the Al–2.3at.%Ge alloy specimens *in situ* irradiation experiments were performed at $T=10$ or 50 K with a flux (ϕ) of 3×10^{19} cm^{-2} s^{-1}, and a total fluence (Φ_{total}) as large as 4.4×10^{23} cm^{-2}.

Two types of irradiation experiments were performed on Ge–Al or Si–Al bilayer specimens at 10 K: (i) the Ge or Si layer of a Ge–Al or Si–Al bilayer specimen faced the direction of the incident electron beam (Fig. 2(a)); or (ii) the Al side of the same bilayer specimen faced the incident beam (Fig. 2(b)). The latter experiment was performed simply by inverting the same specimen. The same flux ($\phi=3\times10^{19}$ cm^{-2} s^{-1}), $T=10$ K and $\Phi_{total}\approx5.3\times10^{23}$ or 6.7×10^{23} cm^{-2} for Ge–Al or Si–Al bilayer specimens respectively were used for both experiments.

We also studied the temperature dependence of Φ_c for an electron-irradiated Ge–Al bilayer specimen. For six different temperatures between 10 and 190 K we used six different areas of the same specimen, *i.e.* for each temperature an area free of radiation damage was utilized. The geometry of Fig. 2(a) was employed for this experiment, as irradiation-induced amorphization of Ge–Al bilayer specimens occurs only for this configuration (see below); $\phi=3\times10^{19}$ cm^{-2} s^{-1} was used at each temperature. At each temperature SADPs were recorded after an increment of fluence ($\Delta\Phi$) of roughly 5×10^{22} cm^{-2}. The value of Φ_c was determined as the Φ value at which diffuse scattering rings first appeared on negatives. SADPs were not recorded unless $\Delta\Phi$ was achieved; the appearance of diffuse scattering rings during an increment of $\Delta\Phi$ was therefore not detectable. The uncertainty in determining Φ_c is approximately $\Delta\Phi/\Phi_c$.

The fluence (cm^{-2}) is converted to the number of displacements per atom (dpa) using tabulated displacement cross-sections [15], and measured displacement threshold energies (T_d) equal to 15, 17 and 16 eV for Ge [16], Si [17, 18] and Al [19] respectively. The value $\Phi=10^{23}$ cm^{-2} corresponds to 10, 6.4 and 6.1 dpa for Ge, Si and Al respectively. Finally, the values of $\Delta\Phi$ are 5, 3.2 and 3.05 dpa for Ge, Si and Al respectively.

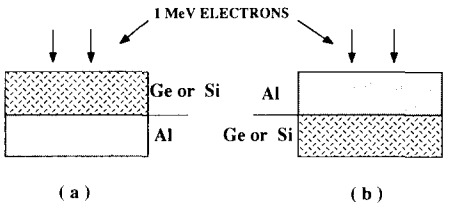

Fig. 2. A schematic diagram illustrating the two configurations of Ge–Al or Si–Al specimens used in our 1 MeV electron beam irradiation experiments: (a) the Ge or Si layer is facing the incident beam; (b) the Al layer is facing the electron beam.

3. Experimental results

3.1. 1 MeV electron irradiation experiments at 10 or 50 K

3.1.1. Two-phase Al–2.3at.%Ge alloy specimens irradiated at 10 or 50 K

Two-phase Al–2.3at.%Ge alloy specimens were irradiated at $T=10$ or 50 K with 1 MeV electrons and $\phi=3\times10^{19}$ cm^{-2} s^{-1}. The dark-field electron micrographs in Fig. 3 illustrate typical results for specimens that had been irradiated at 50 K. The images in Fig.

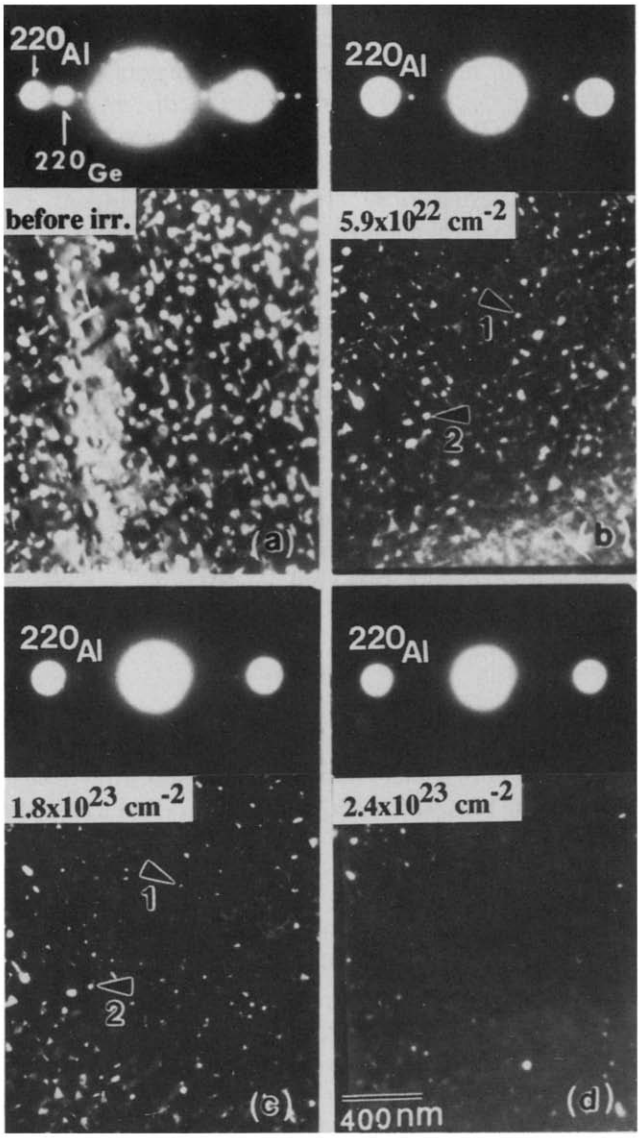

Fig. 3. HVEM dark-field micrographs and their corresponding SADPs of an Al–2.3at.%Ge specimen irradiated to a sequence of fluences at 50 K; the dark-field images were from a Ge (220) diffraction spot as shown in the SADPs: (a) before irradiation; (b) irradiated to 5.9×10^{22}; (c) irradiated to 1.8×10^{23}; (d) irradiated to 2.4×10^{23} cm^{-2}. Note that the intensity of the Ge (220) reflection diminishes with increasing fluence, while the crystalline Ge precipitates gradually disappear from the irradiated zone.

3 were recorded employing the $(220)_{Ge}$ reflection from Ge precipitates, as shown in the accompanying SADPs; each bright spot indicates a Ge precipitate. Figure 3(a) was taken before irradiation, and Figs. 3(b)–3(d) were recorded after irradiating to 5.9×10^{22}, 1.8×10^{23} and 2.4×10^{23} cm^{-2} respectively. Qualitatively the number density and the mean diameter of Ge precipitates decrease gradually, while the intensity of the $(220)_{Ge}$ reflection diminishes slowly with increasing Φ; for comparison, arrows indicating two Ge precipitates are given in Figs. 3(b) and 3(c). The Ge precipitates disappear almost completely from the irradiated zone at $\Phi=2.4\times10^{23}$ cm^{-2} (24 dpa in Ge and 14 dpa in Al). The Ge reflections become very weak at this value; they do not, however, completely disappear from the SADPs for $\Phi_{total}=4.4\times10^{23}$ cm^{-2} (44 dpa in Ge and 27 dpa in Al). These results are qualitatively similar to those reported previously on this alloy [8]. Since diffuse scattering rings are not observed in our experiments, we cannot determine from this type of experiment whether the disappearance of Ge precipitates from the dark-field images is the result of amorphization of Ge precipitates or simply their dissolution induced by electron irradiation. The resolution of this dilemma was obtained from experiments on Ge–Al bilayer specimens that demonstrated that a c-to-a transition occurred at the Ge–Al interface when a bilayer specimen was irradiated at $T=10$ or 50 K with 1 MeV electrons. The absence, therefore, of diffuse scattering rings for an electron-irradiated two-phase alloy specimen is attributed to the fact that the volume fraction of the amorphous phase was not sufficient to cause these rings.

3.1.2. Ge–Al or Si–Al bilayer specimens irradiated at 10 K

Irradiation of a Ge–Al bilayer specimen with 1 MeV electrons at 10 K was found to induce a c-to-a transition only if the Ge side of the bilayer specimen faced the direction of the incident beam: we call this effect *selective amorphization*. Figure 4(a) is a bright-field image of a Ge–Al bilayer specimen before irradiation; the crystalline Al grains (approximately 100 nm in diameter) are in dark contrast. Figure 4(b) is the corresponding SADP; the strong diffraction spots in the SADP are {311}-type reflections from the Ge single crystal layer, while the weak ones, that form concentric rings, are attributable to the vapor-deposited polycrystalline Al layer. For a Si–Al specimen similar micrographs were obtained. Figure 5 exhibits SADPs of the same Ge–Al bilayer specimen irradiated at 10 K with $\phi=3\times10^{19}$ cm^{-2} s^{-1} to $\Phi_{total}=5.3\times10^{23}$ cm^{-2} (53 dpa in Ge and 32 dpa in Al). Figure 5(a) is for the Ge layer facing the direction of the incident beam. Here the appearance of diffuse rings, in comparison with Fig. 4(b), indicates

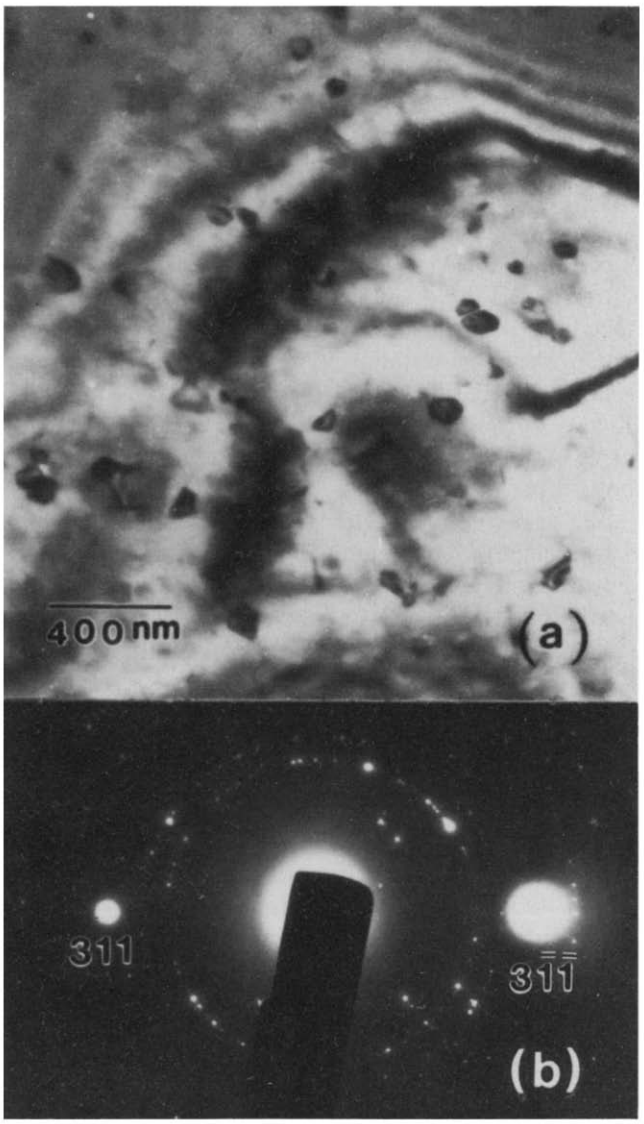

Fig. 4. HVEM images of a Ge–Al bilayer specimen before an irradiation: (a) bright-field electron micrograph showing Al grains on the Ge layer; (b) the corresponding SADP. The indexed strong spots are from Ge single crystal reflections and the weak spots, forming concentric rings, are from the polycrystalline Al layer.

the formation of an amorphous phase in the Ge–Al bilayer. These diffuse rings first appeared at $\Phi_c=2.5\times10^{23}$ cm^{-2} (25 dpa in Ge and 15 dpa in Al) and their intensities increased with increasing fluence. We reported previously a value of $\Phi_c\approx3\times10^{23}$ cm^{-2} [20]; the difference between these two values arises from uncertainty in determining the value of Φ_c. When an Al layer faced the direction of the incident beam (Fig. 5(b)), no diffuse rings were observed for $\Phi_{total}=5.3\times10^{23}$ cm^{-2} (53 dpa in Ge and 32 dpa in Al). We observed that both the Ge and the Al reflections became diffuse because of irradiation-induced secondary defects, *i.e.* a high density of dislocations produced by

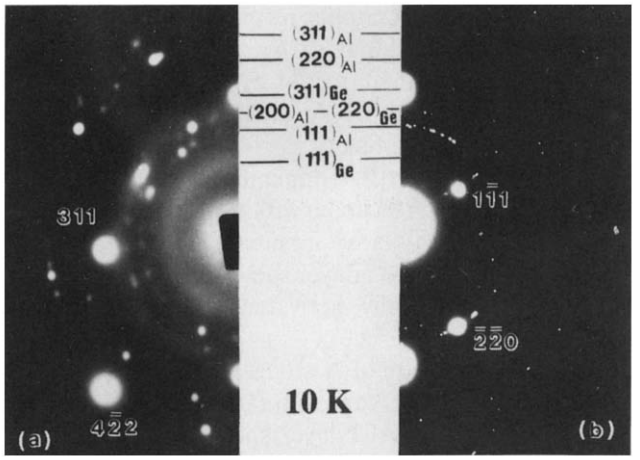

Fig. 5. HVEM SADPs of a Ge–Al bilayer specimen after an irradiation to 5.3×10^{23} cm^{-2} at 10 K. The strong indexed spots are Ge single crystal reflections, while the weak spots forming rings are from the polycrystalline Al layer. (a) The Ge layer faces the incident beam (Fig. 2a); the presence of diffuse scattering rings indicates formation of an amorphous phase. (b) The Al layer faces the incident beam (Fig. 2(b)). No diffuse rings are present.

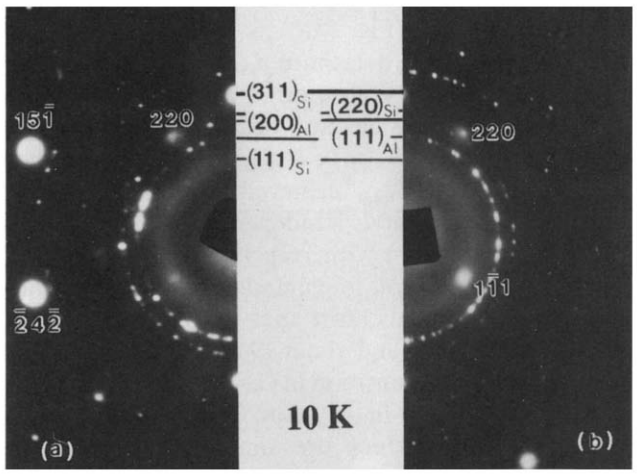

Fig. 6. HVEM SADPs of a Si–Al bilayer specimen after an irradiation to 6.3×10^{23} cm^{-2} at 10 K. The strong indexed spots are Si single crystal reflections, while the weak spots forming rings are from the polycrystalline Al layer. (a) The Si layer faces the incident beam (Fig. 2(a)). (b) The Al layer faces the incident beam (Fig. 2(b)). The presence of diffuse scattering rings is an indication of the formation of an amorphous phase.

the precipitation of mobile SIAs; the mobile SIA is most probably Ge (see below).

A Si–Al bilayer specimen, irradiated at 10 K, exhibited different behavior. Irradiation-induced amorphization occurred in a Si–Al bilayer specimen *independent* of the direction of the incident beam with respect to a specimen. The diffuse rings observed when the Si side of a Si–Al bilayer specimen faced the incident beam (Fig. 6(a)), or *vice versa* (Fig. 6(b)), indicate an amorphous phase. They first appeared at $\Phi_c=3\times10^{23}$ cm^{-2} (19 dpa in Si and 18 dpa in Al), and their intensity increased with increasing Φ; we achieved $\Phi_{total}=6.3\times10^{23}$ cm^{-2} (40 dpa in Si and 38 dpa in Al).

The center of the first diffuse ring in the SADP of an electron-irradiated Ge–Al (Fig. 5(a)) or Si–Al (Figs. 6(a) or 6(b)) bilayer specimen is at a Bragg angle corresponding to the (111) reflection from crystalline Ge or Si, and the center of the second diffuse ring has a spacing between those of the (220) and (311) reflections from crystalline Ge or Si. The diffuse rings in Figs. 5(a), 6(a) or 6(b) constitute diffraction patterns almost identical with those observed for pure amorphous Ge [21] or Si [22] thin films.

An important question is whether the composition of an irradiation-induced amorphous phase in Ge–Al or Si–Al bilayer specimens can be deduced from the difference in the spacings of diffuse rings of an observed amorphous phase and pure amorphous Ge or Si. It was reported previously that amorphous thin films of Ge_xAl_{1-x} ($x\geq0.5$) [21] and Si_xAl_{1-x} ($x\geq0.6$) [22] can be made by a vapor coevaporation technique; the substrate temperature was maintained at room temperature or 77 K during deposition. TEM studies of these amorphous thin films showed that the diffuse scattering rings in SADPs change with the composition of a thin film. The change in the diffuse scattering ring spacings relative to that of a pure Ge or Si amorphous thin film ($x=1.0$) is, however, small, *i.e.* less than 5% in Ge_xAl_{1-x} for $0.5<x\leq1.0$, and less than 3% in Si_xAl_{1-x} for $0.6<x<1.0$. This small effect therefore makes it difficult to deduce precisely the compositions of irradiation-induced amorphous phases by measuring the diameters of diffuse scattering rings.

3.2. Temperature dependence of Φ_c for Ge–Al bilayer specimens in the range 10–190 K

A value of Φ_c exists at which an electron irradiation-induced c-to-a transition is observed in Ge–Al or Si–Al bilayer specimens. To understand this result we studied the temperature dependence of Φ_c for Ge–Al bilayer specimens. Here the Ge side of a bilayer specimen faced the incident beam (Fig. 2(a)); $\phi=3\times10^{19}$ cm^{-2} s^{-1} was used in the range 10–190 K. The results are presented in Fig. 7, where the measurement error in the value of Φ_c is approximately $\pm20\%$ at $\Phi_c\approx2.5\times10^{23}$ cm^{-2}. Note that the value of Φ_c is constant at approximately 2.5×10^{23} cm^{-2} (25 dpa in Ge and 15 dpa in Al) for $T\leq160$ K, and then increases rapidly in the range 160–190 K. The value of Φ_c becomes immeasurably large at a critical temperature (T_c) of 190 K, as no sign of amorphization was detected at $T\approx190$ K for $\Phi_{total}=7\times10^{23}$ cm^{-2} (70 dpa in Ge and 43 dpa in Al); this result is represented in Fig. 7 by a verticle arrow with its origin at $T=190$ K and $\Phi_{total}=7\times10^{23}$ cm^{-2}.

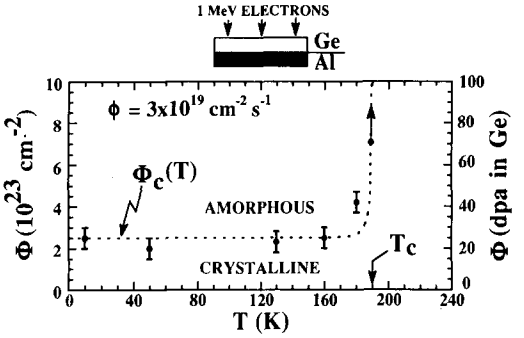

Fig. 7. The variation of the critical fluence for amorphization to occur (Φ_c) with temperature (T) of a Ge–Al bilayer specimen subjected to 1 MeV electron irradiation at a constant flux (ϕ) of 3×10^{19} cm^{-2} s^{-1}. The Ge layer of the bilayer specimen faces the incident beam. No amorphization is observed above a critical temperature (T_c) of roughly 190 K. The calculated Φ_c as a function of T is denoted by the dashed curve (see Section 4.2 for the details of the model used to calculate this curve).

4. Discussion

4.1. Recoil implantation effects in Ge–Al or Si–Al bilayer specimens

We now discuss the amorphization of Ge–Al or Si–Al bilayer specimens induced by electron irradiation at 10 K in terms of the elastic collision processes that occur when energetic electrons encounter atoms of a bilayer specimen. During an electron irradiation a fraction of the kinetic energy of an incident electron is transferred to an atom of the layer facing the incident beam, layer A. An A atom in the interface region may recoil into the bottom layer, layer B, if the energy transferred to an A atom is greater than the minimum energy required to displace it permanently from its lattice site (T_d). In this manner A atoms are implanted into layer B via a recoil mechanism. We employed the TRIM-88 Monte Carlo code [23] to simulate the range profile of Ge in Al employing an incident Ge ion energy of 60 eV; this yielded a mean range of 0.9 nm and a straggling of 0.2 nm. The total displacement cross-section for an A atom (σ_A) is a function of T_d, the kinetic energy of the incident electrons (E), the atomic number (Z), and the atomic mass (M) of the recoiling A atoms. For $E \gg mc^2 = 0.511$ MeV (the energy of an electron associated with its rest mass) σ_A is given by:

$$\sigma_A \sim \frac{2\pi}{T_d}\frac{Z^2e^4}{Mc^2} = (1.4\times10^{-22})\frac{Z^2}{T_dN}\ (\text{cm}^2) \qquad (1)$$

where e is the charge on an electron, c the speed of light and N the atomic mass number [24]. If we take $N \approx 2Z$ then σ_A is directly proportional to Z. For a 1 MeV electron irradiation eqn. (1) gives an approximate value of σ_A. We obtain the ratios $\sigma_{Ge}/\sigma_{Al} \approx 2.4$ and $\sigma_{Si}/\sigma_{Al} \approx 1.1$ with $Z = 32$, 14 and 13; $N = 72.6$, 28 and 27; and $T_d = 15$, 17 and 16 eV for Ge, Si and Al respectively. Taking the flux of A atoms recoiling into the layer B ($J_{A/B}$) to be proportional to σ_A, it follows that $J_{Ge/Al}$ is approximately equal to 2.4 $J_{Al/Ge}$ and $J_{Si/Al}$ is approximately equal to 1.1 $J_{Al/Si}$. Therefore, for Ge–Al bilayer specimens the flux of recoiling atoms is different by a factor of about 2.4 depending on the direction of the incident electron beam with respect to a specimen, while $J_{Si/Al}$ or $J_{Al/Si}$ is approximately independent of orientation for a Si–Al bilayer specimen. The diffusional effects, both thermally activated and athermal, are discussed below.

Recoil implantation of A atoms into the layer B leads to the formation of a supersaturated solid-solution for both Ge–Al and Si–Al bilayer specimens, as the solid solubility of Ge or Si in Al and *vice versa* is extremely small (less than 0.01 at.%) for $T < 300$ K [25]. The concentration of A atoms in the supersaturated solid-solution, c_A, is proportional to $J_{A/B}$. If we assume that a c-to-a transition takes place when c_A exceeds a critical value $c_{A/B}^{Crit}$, which is related to Φ_c at temperature, our experimental results can be accounted for in terms of the difference between $J_{A/B}$ and $J_{B/A}$. For Ge–Al bilayer specimens the value of Φ_c when the Ge layer faces the incident beam (Fig. 2(a)) is smaller than in the inverse case (Fig. 2(b)), since $J_{Ge/Al}$ is approximately equal to $2.4J_{Al/Ge}$. The absence of amorphization when an Al layer faces the electron beam may be attributed to a low value of $J_{Al/Ge}$, *i.e.* $c_{Al/Ge}^{Crit}$ cannot be reached for the value of Φ_{total} achieved. For Si–Al bilayer specimens the value of Φ_c is independent of the direction of the incident beam with respect to a bilayer as $J_{Si/Al} \approx 1.1J_{Al/Si}$. The recoil-implantation mechanism is further supported by the fact that a large value of Φ_c (about 25 dpa in Ge and about 19 dpa in Si) is required to observe a c-to-a transition in Ge–Al and Si–Al bilayer specimens, and also in Al–2.3at.%Ge two-phase alloy specimens; these values are simply too high to be consistent with the vacancy-accumulation mechanism postulated in ref. 8. The high values of Φ_c are a result of electron-beam stimulated migration of recoil-implanted Ge atoms in Al via a monovacancy mechanism: see Section 4.4 below.

We have assumed that $c_{Al/Ge}^{Crit} \approx c_{Ge/Al}^{Crit}$ and $c_{Al/Si}^{Crit} \approx c_{Si/Al}^{Crit}$, *i.e.* the critical concentration of Al in Ge or Si is equal to that of Ge or Si in Al. In fact, $c_{A/B}^{Crit}$ need not be equal to $c_{B/A}^{Crit}$, as for Ge–Al bilayer specimens the selective amorphization effect is favored if $c_{Al/Ge}^{Crit} > c_{Ge/Al}^{Crit}$. For amorphous thin films of Ge_xAl_{1-x} or Si_xAl_{1-x} alloys prepared by vapor codeposition the value of $c_{A/B}^{Crit}$ was deduced from TEM observations [21, 22]. It was found that $c_{Al/Ge}^{Crit} \approx 0$ and $c_{Ge/Al}^{Crit} \approx 50$ at.%Ge for Ge_xAl_{1-x} alloys; and $c_{Al/Si}^{Crit} \approx 0$ and $c_{Si/Al}^{Crit} \approx 60$ at.% Si for Si_xAl_{1-x} alloys. Thus Ge or Si can be vapor-deposited in an amorphous state without Al, while a significant Ge or Si concentration is required to render

Al amorphous. We argue, however, that the value of $c^{Crit}_{Ge/Al}$ or $c^{Crit}_{Si/Al}$ should depend on the experimental conditions under which a thin film is prepared, *e.g.* the substrate temperature and the deposition rate.

Based on the atomic size effect an empirical model has been proposed to calculate $c^{Crit}_{A/B}$ for metal–metal and metal–metalloid systems [26]. Taking the atomic radii of Ge, Si and Al to be 0.122, 0.118 and 0.143 nm respectively, this model yields $c^{Crit}_{Al/Ge}=0.16$ at.% Al and $c^{Crit}_{Ge/Al}=0.26$ at.% Ge for the Ge–Al system; and $c^{Crit}_{Al/Si}=0.13$ at.% Al and $c^{Crit}_{Si/Al}=0.23$ at.% Si for the Si–Al system. These values are quite different from the experimental values obtained for vapor-deposited thin films of the Ge–Al and Si–Al systems. In this model the value of $c^{Crit}_{A/B}$ is sensitive to the atomic size ratio between atoms A and B. Since the atomic size depends upon the composition and the structure of alloys, the determination of the size factor of an element is ambiguous and sometimes misleading, in particular when a metalloid element is involved. In conclusion, we are not able to make a definitive estimate of $c^{Crit}_{A/B}$ for the Ge–Al or Si–Al bilayer systems.

4.2. A phenomenological model to explain the temperature dependence of Φ_c

The temperature dependence of Φ_c for the Ge–Al bilayer specimens (Fig. 7) can be accounted for in terms of the mobility of the recoil-implanted Ge atoms in an Al matrix employing a phenomenological model. During an electron irradiation with a flux ϕ, the accumulation rate of Ge atoms at a given depth in the Al layer is determined by two factors. The first is the recoil implantation of the Ge atoms. This causes an accumulation of Ge atoms at a rate α that is a constant for a given ϕ. The second is the temperature-dependent mobility of Ge atoms. This results in a decrease in the accumulation rate of Ge atoms. (We do not explicitly include the temperature-independent electron-beam stimulated migration of Ge atoms in Al in this model as it is included in α: see Sections 4.3 and 4.4.) The steady-state value of c_{Ge} results from a competition between these two factors, and amorphization occurs when the resultant c_{Ge} exceeds $c^{Crit}_{Ge/Al}$; as discussed in Section 4.1 we do not *a priori* know the value of $c^{Crit}_{Ge/Al}$. If we ignore the effect of the concentration gradient of the Ge atoms in the Al matrix, then a phenomenological rate equation for c_{Ge} may be written as:

$$\frac{dc_{Ge}}{dt} = \alpha - \nu c_{Ge} \tag{2}$$

where ν is the temperature dependent jump frequency of a Ge atom. If Ge atoms diffuse via a single thermally activated mechanism then ν is given by:

$$\nu = \nu_0 e^{-h^m_{Ge}/kT} \tag{3}$$

where ν_0 is the 'attack' frequency of the Ge atoms (it is within an order of magnitude of the Debye frequency for Al), h^m_{Ge} is the activation enthalpy for the migration of the Ge atoms, and k is Boltzmann's constant. It should be noted that no terms for point defects (vacancies or SIAs) are introduced explicitly in eqn. (2). The reason for this is that the mean range of the recoil-implanted Ge atoms is very small (about 0.9 nm) and the range profile is highly localized (the straggling distance is 0.2 nm) in the region just below the Ge–Al interface. The Ge atoms sit in a uniform sea of vacancies and SIAs; the steady-state concentrations of vacancies and SIAs are determined by the recombination volumes and diffusivities of these point defects at a given irradiation temperature. The above physical picture cannot be described by the usual rate equations of radiation-enhanced diffusion which assume that the point defects, the solute atoms and point defect sinks are uniformly distributed in an infinite space; see refs. 27–29. We therefore use this simple phenomenological rate equation, eqn. (2), and describe the migration of the Ge atoms by eqn. (3).

With the initial condition that $c_{Ge}=0$ when $t=0$, the solution of eqn. (2) is:

$$c_{Ge}(t) = \frac{\alpha}{\nu}(1-e^{-\nu t}) \tag{4}$$

For $t\to\infty$ the steady-state concentration is:

$$c_{Ge}(\infty) = \frac{\alpha}{\nu} = \frac{\alpha}{\nu_0} e^{h^m_{Ge}/kT} \tag{5}$$

This shows that $c_{Ge}(\infty)$ decreases as temperature increases because the mobility of the Ge atoms increases exponentially with increasing temperature. An equation for the temperature dependence of the irradiation fluence, $\Phi(T)$, necessary to cause amorphization can be derived by using the relation $\Phi=\phi t$. The critical fluence Φ_c follows from $c_{Ge}(t)=c^{Crit}_{Ge/Al}$, i.e.:

$$\Phi_c = -\frac{\phi}{\nu}\ln\left(1-c^{Crit}_{Ge/Al}\frac{\nu}{\alpha}\right) \tag{6}$$

Substituting eqn. (3) into eqn. (6) yields Φ_c as a function of temperature. At low temperatures $\nu/\alpha \ll 1$, and eqn. (6) becomes:

$$\Phi_c \approx \frac{\phi}{\alpha} c^{Crit}_{Ge/Al} \tag{7}$$

In the low temperature range, therefore, Φ_c is independent of temperature, as observed experimentally. In our experiments $\Phi_c = 2.5\times10^{23}$ cm^{-2} for $T<160$ K and $\phi = 3\times10^{19}$ cm^{-2} s^{-1}, and we therefore obtain from eqn. (7):

$$c^{\mathrm{Crit}}_{\mathrm{Ge/Al}}/\alpha = \Phi_c/\phi = 8.333\times10^3 \text{ s} \quad (8)$$

According to eqns. (3) and (6) there is a critical temperature, T_c, at which

$$(c^{\mathrm{Crit}}_{\mathrm{Ge/Al}}/\alpha)\nu_0 e^{-h^{\mathrm{m}}_{\mathrm{Ge}}/kT_c} = 1 \quad (9)$$

this equation leads to $\Phi_c \to \infty$. T_c is the critical temperature above which the steady-state concentration, $c_{\mathrm{Ge}}(\infty)$, cannot reach $c^{\mathrm{Crit}}_{\mathrm{Ge/Al}}$ and, consequently, for $T \geq T_c$ a c-to-a transition cannot be observed during irradiation. For our experimental data we find $T_c = 190$ K. Using eqns. (8) and (9), and $\nu_0 \approx 10^{13}$ s^{-1}, the value of the activation enthalpy for the migration of Ge atoms can be extracted from eqn. (9), *i.e.* $h^{\mathrm{m}}_{\mathrm{Ge}} \approx 0.64$ eV. Interestingly, this value is approximately equal to the migration enthalpy of an Al monovacancy, $h^{\mathrm{m}}_{\mathrm{lv}} = 0.65$ eV, determined from the recovery behavior of quenched-in monovacancies [30], and close to a 'best' value of $h^{\mathrm{m}}_{\mathrm{lv}}$ (0.62 eV) [31].

The parameters in eqns. (3) and (6) are listed in Table 1; the values of these parameters were used to calculate $\Phi_c(T)$ numerically and the results are shown in Fig. 7 (the dashed curve). We note that $\Phi_c(T)$ remains constant for a wide temperature range, 0 to about 180 K, and then abruptly increases with increasing temperature. The value of $\Phi_c(T)$ becomes immeasurably large at $T = 190$ K. This phenomenological model is, therefore, in good agreement with the experimental results. Note that the predicted change in $\Phi_c(T)$ as T approaches T_c is more abrupt than the experimental data; this is expected for a single thermally activated mechanism. If we introduce a second activation enthalpy for migration, *e.g.* allow for migration of germanium atoms via a divacancy mechanism, and consider the effect of a Ge concentration gradient, arising from a recoil-implantation profile, then a broader $\Phi_c(T)$ *vs.* T curve is expected.

The results and above interpretation of the amorphization effects observed for Ge–Al bilayer specimens explain the dilemma presented by the results of ref. 8 and our results described in Section 3.1.1. In this experiment the Ge precipitates are slowly dissolving because of an electron irradiation. The dissolution process results in the amorphization of the surrounding Al matrix, but this amorphized material is difficult to observe in SADPs because of the small volume fraction of specimen affected. Alternatively the amorphization process can be monitored in the SADPs employing a bilayer geometry, because of the larger volume fraction of specimen affected.

4.3. Interpretation of the activation enthalpy $h_{Ge}{}^{m}$ in terms of a point defect mechanism and radiation-enhanced diffusion of recoil-implanted Ge atoms

In electron-irradiated pure Al specimens Stage I_E recovery, which is now widely attributed to long-range uncorrelated migration of aluminum SIAs, occurs between about 43 and 50 K [32, 33]. Since no change in the value of Φ_c is observed in this temperature range we conclude that Al SIAs do *not* play a role in the c-to-a transition as the Al SIA is freely mobile throughout the range 50–190 K. The Ge or Si SIAs are also freely mobile (a Stage I recovery peak has *never* been observed for electron-irradiated pure Ge or Si) in the range 10–190 K [34]; therefore neither Ge nor Si SIAs play an important role in the c-to-a transitions we observed.

Stage II recovery in quenched Al occurs between 200 and 350 K, while in electron-irradiated Al Stage III recovery occurs in the range 200–250 K; see ref. 31 for a review of the critical experiments. Stage III recovery in quenched or irradiated Al is generally attributed to the long-range migration of vacancies. Therefore, we now consider several relevant experiments on Stage III recovery in irradiated or quenched pure Al. The value of T_c we observed is somewhat below the temperature (228 K) at which a large isochronal annealing stage was found in an Al specimen that had been irradiated at 90 K with 2 MeV electrons [35]. The latter researchers [35] determined an activation enthalpy of 0.62 ± 0.04 eV for the recovery peak at 228 K, and attributed it to the migration of monovacancies by comparison of this activation enthalpy with the value observed for quenched and annealed Al [36]. The details of Stage III recovery behavior of quenched Al are dependent on the quench temperature (T_q). At a T_q of 773 K a low temperature recovery peak at about 213 K dominates, with an activation enthalpy between 0.44 and 0.50 eV, while for $T_q = 573$ K a single recovery peak occurs at 293 K with an activation enthalpy of

TABLE 1. The parameters and their values used for numerical calculations of the critical fluence (Φ_c) as a function of temperature (T)

Parameters	Symbol	Value
Electron irradiation fluence	ϕ	3×10^{19} cm^{-2} s^{-1}
Critical fluence at 10 K	Φ_c	2.5×10^{23} cm^{-2}
Ge atom attack jump frequency in Al	ν_0	$\approx 10^{13}$ s^{-1}
Activation enthalpy for Ge atom migration in Al under irradiation	$h^{\mathrm{m}}_{\mathrm{Ge}}$	0.64 eV[a]

[a]This value was determined by fitting the phenomenological model to the experimental data exhibited in Fig. 7.

0.65 eV [30]. The reason for this difference between the two values of T_q is that at high T_q a large concentration of divacancies is quenched-in along with the monovacancies, and divacancies are considerably more mobile than monovacancies [30, 31].

The relevant tracer diffusion data for the Al and Al(Ge) systems under thermal equilibrium conditions [37] are listed in Table 2. The activation enthalpies in the expressions for the tracer diffusivities are the same, 1.26 eV, indicating that the binding free energy of a monovacancy–germanium pair is negligible. Regarding the migration of Ge atoms in an Al matrix the effective monovacancy jump frequency is not affected by the presence of Ge atoms, since the binding free energy between Ge atoms and Al monovacancies is very small [40, 41]. Consequently, the activation enthalpy for the diffusion of Ge atoms, via a monovacancy mechanism, is nearly identical with the activation enthalpy for self-diffusion of Al atoms via a monovacancy mechanism. Therefore we do not need to consider the binding free energy of a monovacancy to a Ge atom in discussing our results.

During irradiation without a mobile vacancy population, accumulation of Ge atoms with a range profile occurs in the Al at a temperature-independent rate; strictly speaking this is a first-order approximation because of the electron-beam stimulated migration of Ge atoms in Al (see Section 4.4). Consequently, c_{Ge} steadily increases and reaches $c^{Crit}_{Ge/Al}$; therefore, Φ_c remains constant between about 10 and 160 K. As the temperature approaches T_c, Ge atoms become mobile because of the thermally activated migration of Al vacancies. This leads to a decrease in the accumulation rate of Ge atoms and, therefore, an increase in Φ_c. For $T \geq T_c$ the mobility of Ge atoms is sufficiently large to prevent c_{Ge} from reaching $c^{Crit}_{Ge/Al}$ and, therefore, no amorphization occurs.

The monovacancy mechanism for the migration of Ge atoms is also implied by the fact that the activation enthalpy for Ge migration, $h^m_{Ge} = 0.64$ eV, is nearly equal to the migration enthalpy of Al vacancies, $h^m_{lv} = 0.62$ eV [31] or 0.65 eV [30]. The only remaining question is why did we observe an activation enthalpy of 0.64 eV in the range 180–190 K, whereas in ref. 30 this activation enthalpy is observed at considerably higher temperatures. The answer to this question lies with the fact that the number of jumps (n_j) of a Ge atom required to reduce the Ge supersaturation necessary for amorphization is small because of the narrow range profile of the recoil-implanted Ge atoms and their proximity to the Ge–Al interface.

The diffusivity of a monovacancy, $D_{lv}(T)$, in Al is given by the tracer diffusion coefficient, D_T, divided by the thermal equilibrium vacancy concentration, c_{lv}:

$$D_{lv}(T) \approx 0.055 \exp(-0.60\ eV/kT)\ \text{cm}^2\ \text{s}^{-1} \quad (10)$$

based on D_T data [37] and a critical evaluation of c_{lv} for Al [42]. Equation (10) yields a value of D_{lv} equal to 6.7×10^{-18} cm^2 s^{-1} at 190 K. The activation enthalpy in the Boltzmann factor of eqn. (10), 0.60 eV, is slightly less than a 'best' value of the enthalpy of migration of a monovacancy of 0.62 eV [31]. This difference is most probably the result of uncertainties in the Boltzmann factors for D_T and c_{lv}. The radiation-enhanced diffusivity of a Ge atom in Al, D'_{Ge}, is the product of this $D_{lv}(T)$ and the steady-state monovacancy concentration, c'_{lv}, at the same temperature, in the region of the Ge implantation profile where the Ge atoms are mobile, *i.e.* $D'_{Ge} = c'_{lv} D_{lv}(T)$. If we take c'_{lv} to be the saturation vacancy concentration, 2.8×10^{-3} at.fr., for electron-irradiation induced Frenkel pairs in pure Al [43] then the root mean squared radiation-enhanced diffusion distance of a Ge atom in Al at 190 K is 0.31 nm for 8333 s; the latter is the time to accumulate Φ_c between 10 and 160 K. This distance is approximately 1/3 of the mean range (0.9 nm) of the recoil-implanted Ge atoms and 1.6 times the straggling distance (0.2 nm), therefore the radiation-enhanced diffusion of Ge atoms at 190 K can partially help to explain the suppression of the c-to-a transition at this temperature, although, as discussed in Section 4.4, there is also an important athermal contribution from the electron-beam stimulated migration of Ge atoms in Al.

4.4. Electron-beam stimulated migration of recoil-implanted Ge atoms in Al

An additional process that contributes to the suppression of the c-to-a transition is electron-beam stimulated

TABLE 2. Point defect properties for pure Al, and tracer diffusion data for the Al and Al(Ge) systems at thermal equilibrium

Parameters	Notation	Value (eV)	Ref.
Al monovacancy formation enthalpy	h^f_{lv}	0.69	38
Al monovacancy migration enthalpy	h^m_{lv}	0.65	30
"Best value" of the Al monovacancy migration enthalpy	h^m_{lv}	0.62	31
Al self-interstitial atom migration enthalpy	h^m_{li}	0.115	39
Tracer self-diffusion activation enthalpy for Al in Al	h_{th}	1.26	37
Tracer activation enthalpy for Ge atom diffusion in Al	h^{Ge}_{th}	1.26	37

migration of Ge atoms in an Al matrix [10, 11]. In this mechanism the migration of a Ge atom occurs if it receives a transferred energy greater than h^{m}_{Ge} from the 1 MeV electron beam, and if vacancies exist in the first nearest-neighbor shell of atoms surrounding a Ge atom. The electron-beam stimulated migration mechanism is discussed in detail in the Appendix, where it is shown that the root mean squared diffusion distance arising from this mechanism is 1.57 nm for $t=8333$ s independent of temperature. Between 10 and 160 K the main effect of the electron-beam stimulated migration of Ge atoms is to determine the value of Φ_c required for the c-to-a transition. This is because the electron-beam stimulated migration of Ge atoms decreases the rate at which the critical concentration of Ge necessary for a c-to-a transition is reached. It therefore increases the value of Φ_c necessary for a c-to-a transition over the value required without electron-beam stimulated migration of Ge atoms. In the range where radiation-enhanced diffusion becomes significant the total root mean squared diffusion distance of Ge atoms resulting from these two mechanisms is large enough to suppress completely the c-to-a transition. The total value of the root mean squared diffusion distance at 190 K for the two mechanisms is about 2 nm, and this is 2.2 times the mean range of a recoil-implanted Ge atom (0.9 nm) and ten times the straggling distance (0.2 nm). Thus we conclude that both the radiation-enhanced diffusion and electron-beam stimulated migration of Ge atoms in Al play important roles in the suppression of the c-to-a transition at 190 K.

5. Summary

Experiments were performed in the temperature range 10–190 K employing the 1 MeV high voltage electron microscope at the Argonne National Laboratory. The purpose of these experiments is to elucidate the mechanism of the crystalline to amorphous (c-to-a) transition below 190 K, and also the suppression of the c-to-a transition above 190 K, in two-phase Al(Ge) alloys, and Ge–Al or Si–Al bilayer specimens.

(i) Two-phase Al–2.3at.%Ge alloy specimens were irradiated at $T=10$ or 50 K with 1 MeV electrons and $\phi=3\times10^{19}$ cm^{-2} s^{-1}. Qualitatively the mean number density and the mean diameter of the pure Ge precipitates decreases with increasing fluence (Φ), while the intensity of the $(220)_{Ge}$ reflection diminishes slowly with increasing Φ; see the two Ge precipitates indicated by arrows in Figs. 3(b) and 3(c). At $\Phi=2.4\times10^{23}$ cm^{-2} (24 dpa in Ge and 14 dpa in Al) the Ge precipitates disappear almost completely from the electron-irradiated zone. Also, at this value of Φ the $(220)_{Ge}$ reflections are weak but still present. For a total fluence (Φ_{total}) of 4.4×10^{23} cm^{-2} (44 dpa in Ge and 27 dpa in Al) the $(220)_{Ge}$ reflections do not completely disappear from the selected area diffraction patterns (SADPs). These results are qualitatively similar to those reported previously on the same alloy [8]. Since diffuse scattering rings are not observed in the SADPs, we cannot determine from this type of experiment whether the disappearance of Ge precipitates from the dark-field images is the result of the amorphization of Ge precipitates or simply their dissolution induced by electron irradiation.

(ii) The resolution of the dilemma described in (i) was obtained from experiments on Ge–Al bilayer specimens which demonstrated that a c-to-a transition occurs at the Ge–Al interface when a bilayer specimen is irradiated at $T=10$ or 50 K with 1 MeV electrons. The geometry of the specimens employed to observe this transition is displayed in Fig. 2(a). When a Ge layer faces the incident electron beam, diffuse rings in a SADP first appeared at a critical fluence of $\Phi_c=2.5\times10^{23}$ cm^{-2} (25 dpa in Ge and 15 dpa in Al). When an Al layer faces the incident electron beam (Fig. 5(b)) no diffuse rings were observed for $\Phi_{total}=5.3\times10^{23}$ cm^{-2} (53 dpa in Ge and 32 dpa in Al). We did, however, observe that both the Ge and Al reflections became diffuse because of irradiation-induced secondary defects, *i.e.* a high density of dislocations caused by the precipitation of mobile SIAs; the most likely SIA is the Ge SIA (see Section 4.3). The asymmetry in the c-to-a transition (Ge layer facing the incident electron beam *vs.* the Al layer facing the electron beam) is denoted a selective amorphization effect.

(iii) A Si–Al bilayer specimen, irradiated at 10 K, exhibited a different behavior from a Ge–Al bilayer specimen. Irradiation-induced amorphization occurs in a Si–Al bilayer specimen independent of the direction of the incident beam with respect to a bilayer. The critical fluence for amorphization to occur in this system is $\Phi_c=3\times10^{23}$ cm^{-2} (19 dpa in Si and 18 dpa in Al).

(iv) The results for the Ge–Al and Si–Al bilayer specimens are explained by an electron irradiation-induced recoil-implantation process, where the amorphization occurs because of a change of chemistry of the pure element caused by a recoil-implantation process. The asymmetry between the Ge–Al and Si–Al results can be understood by considering the total displacement cross-section for transferring sufficient kinetic energy to an atom to displace it permanently from a top layer into a bottom layer, *e.g.* from Ge to Al and *vice versa* or from Si to Al and *vice versa*. This cross-section is approximately directly proportional to the atom number (Z). If we take the ratio of the cross-sections to be proportional to the ratio of the atomic fluxes (J) from one layer into a second layer it follows

that $J_{Ge/Al}$ is approximately equal to $2.4J_{Al/Ge}$ and $J_{Si/Al}$ is approximately equal to $1.1J_{Al/Si}$ (see Section 4.1). Therefore, for Ge–Al bilayer specimens the flux of recoiling atoms is different by a factor of about 2.4, dependent on the direction of the incident electron beam with respect to a specimen, while $J_{Si/Al}$ or $J_{Al/Si}$ is approximately independent of orientation for a Si–Al bilayer specimen. The chemistry of the Ge–Al and Si–Al systems must be such that is more difficult to amorphize Ge by adding Al to it than it is to amorphize Si by adding Al to it via recoil-implantation processes.

(v) The above results explain the dilemma presented by the results of ref. 8 and our results described in (i). In this experiment the Ge precipitates are dissolving slowly because of electron irradiation. The dissolution process results in the amorphization of the surrounding Al matrix, but this amorphization effect is difficult to observe in SADPs because of the small volume fraction of a specimen affected. Alternatively the amorphization process can be detected in the SADPs employing a bilayer geometry because of the larger volume fraction of a specimen affected.

(vi) The temperature dependence of Φ_c for a Ge–Al specimen was studied for the situation where the Ge side faces the incident electron beam. It was found that Φ_c remains constant in the temperature range 10–160 K, then Φ_c increases rapidly with increasing T in the range 160–190 K, and finally becomes immeasurably large (greater than 70 dpa in Ge and greater than 43 dpa in Al) at $T=T_c=190$ K; T_c is the critical temperature above which no amorphization can be observed: see Fig. 7.

(vii) In terms of the mobility of the recoil-implanted Ge atoms in the Al matrix, our results are qualitatively accounted for by a phenomenological rate-theory model (see Section 4.2) in which the migration of Ge atoms during an irradiation occurs with an effective activation enthalpy $h^m_{Ge}=0.64$ eV; this value of h^m_{Ge} is close to the migration enthalpy of a monovacancy in pure Al (0.62 [31] or 0.65 eV [30]): see Table 2. Since h^m_{Ge} is nearly equal to the migration enthalpy of a monovacancy in Al, this may be understood in terms of the radiation-enhanced diffusion of Ge atoms occurring in the presence of a very high monovacancy concentration produced by the 1 MeV electron irradiation. In addition, the contribution to the diffusion of Ge atoms in Al from electron-beam stimulated migration of Ge atoms is considered: see Section 4.4 and the Appendix. It is demonstrated quantitatively that the root mean squared diffusion distance of Ge atoms in Al at 190 K resulting from a thermally activated radiation-enhanced monovacancy diffusion mechanism plus the athermal electron-beam stimulated migration of Ge atoms in Al is about 2 nm; this distance is approximately 2.2 times the mean range of 0.9 nm of recoil-implanted Ge atoms in Al, and 10 times the straggling distance of 0.2 nm of Ge in Al.

Acknowledgments

X.W.L. received partial support from the Robert R. McCormick School of Engineering and Applied Science for this research. This work made use of central facilities supported by the National Science Foundation through Northwestern University's Materials Research Center, grant No. DMR-8821571. This research was made possible by the use of the High Voltage Electron Microscope Facility at Argonne National Laboratory. The aid of Messrs. E. Ryan and S. Ockers of this facility is gratefully acknowledged. P.R.O. was supported by the US Department of Energy, BES-MS, under contract number W-31-109-Eng-38. D.N.S. wishes to thank Dr. G. Martin for useful discussions and kind hospitality at Centre d'Etudes de Saclay (D.Tech/S.R.M.P.) that was made possible by a National Science Foundation US-France Cooperative Science grant No. INT-871532 (Dr. Christine Glenday, grant officer).

References

1 N. Sumida and H. Fujita, in H. Fujita (ed.), *International Symposium on In Situ Experiments with HVEM*, Osaka University Press, 1985, p. 477.
2 M. D. Matthews and S. J. Ashby, *Philos. Mag., 27* (1973) 1313.
3 H. Föll, in F. A. Huntley (ed.), *Lattice Defects in Semiconductors*, IOP Conference Proceedings No. 23, Institute of Physics, Bristol, 1975, p. 233.
4 D. N. Seidman, R. S. Averback, P. R. Okamoto and A. C. Baily, *Mat. Res. Soc. Symp. Proc., 51* (1986) 349.
5 D. N. Seidman, R. S. Averback, P. R. Okamoto and A. C. Baily, *Phys. Rev. Lett., 58* (1987) 900.
6 F. L. Vook, in *Radiation Damage and Defects in Semiconductors*, Institute of Physics, London, 1972, p. 60.
7 L. A. Cristel, J. F. Gibbons and T. W. Sigmon, *J. Appl. Phys., 52* (1981) 7143.
8 K. L. Rusbridge, *Radiat. Effects, 69* (1983) 277.
9 H. Mori, S. Nakamura and H. Fujita, in T. Imura, S. Maruse and T. Suzuki (eds.), *Proceedings of the XIth International Congress on Electron Microscopy*, Japanese Society of Electron Microscopy, Tokyo, 1986, p. 1113.
10 R. S. Nelson, *Philos. Mag., 10* (1964) 723.
11 K. Urban and A. Seeger, *Philos. Mag., 30* (1974) 1395.
12 U. Köster, *Mater. Sci. Eng., 5* (1969/70) 174.
13 G. R. Hugo and B. C. Muddle, *Acta Metall. Mater., 38* (1990) 351.
14 K. Haga, W. E. King, K. L. Merkle and M. Meshii, *Nucl. Instrum. Methods B, 16* (1986) 134.
15 O. Oen, Oak Ridge National Laboratory Report No. 4897, Solid State Sciences Division, 1973.
16 C. A. Ferreira-Lima and A. Howie, *Philos. Mag., 34* (1976) 1057.
17 J. J. Loferski and P. Rappaport, *J. Appl. Phys., 30* (1959) 1296.
18 R. L. Novak, *Bull. Am. Phys. Soc., 8* (2) (1963) 235.

19 P. Vajda, *Rev. Mod. Phys., 49* (1977) 481.
20 X. W. Lin, J. Koike, D. N. Seidman and P. R. Okamoto, *Philos. Mag. Lett., 60* (1989) 233.
21 U. Köster, *Acta Metall., 20* (1972) 1361.
22 U. Köster and P. Weiss, *J. Non-Cryst. Solids, 17* (1975) 359.
23 J. F. Ziegler, J. P. Biersack and V. Littmark, *The Stopping Powers and Ranges of Ions in Solids*, vols. I and II, Pergamon, New York, 1986.
24 J. W. Corbett, in F. Seitz and D. Turnbull (eds.), *Solid State Phys., 7* (supplement), Academic Press, New York, 1966.
25 A. J. McAlister and J. L. Murray, *Bull. Alloy Phase Diagrams, 5* (1984) 74, 341.
26 T. Egami and Y. Waseda, *J. Non-Cryst. Solids, 64* (1984) 113.
27 G. J. Dienes and A. C. Damask, *J. Appl. Phys., 29* (1958) 1713.
28 N. Q. Lam and S. J. Rothman, in N. L. Peterson and S. J. Rothman (eds.), *Radiation Damage in Metals*, American Society for Metals, Metals Park, OH, 1976, pp. 125–156.
29 R. Sizmann, *J. Nucl. Mater., 69&70* (1978) 386.
30 V. Lévy, J. M. Lanore and J. Hillairet, *Philos. Mag., 28* (1973) 373.
31 R. W. Balluffi, *J. Nucl. Mater., 69&70* (1978) 240.
32 R. L. Chaplin and H. M. Simpson, *Phys. Rev., 163* (1967) 587.
33 W. Schilling, G. Burger, K. Isebeck and H. Wenz, in A. Seeger, D. Schumacher, W. Schilling and J. Diehl (eds.), *Vacancies and Interstitials in Metals*, North-Holland, Amsterdam, 1970, p. 255.
34 J. W. Corbett, J. P. Karins and T. Y. Tan, *Nucl. Instrum. Methods, 182/183* (1981) 457.
35 Y. N. Lwin, M. Doyama and J. S. Koehler, *Phys. Rev., 165* (1968) 787.
36 M. Doyama and J. S. Koehler, *Phys. Rev., 134* (1964) A522.
37 N. L. Peterson and S. J. Rothman, *Phys. Rev. B, 1* (1970) 3264.
38 P. Tzanetakis, J. Hillairet and G. Revel, *Phys. Status Solidi B, 75* (1976) 433.
39 H. M. Simpson and R. L. Chaplin, *Phys. Rev., 178* (1969) 1166.
40 T. R. Anthony, *Acta Metall., 18* (1970) 307.
41 R. W. Balluffi and P. S. Ho, in *Diffusion*, American Society For Metals, Metals Park, OH, 1973, p. 83.
42 R. W. Siegel, *J. Nucl. Mater., 69&70* (1978) 117.
43 M. W. Thompson, *Defects and Radiation Damage in Metals*, Cambridge University Press, Cambridge, 1969, pp. 253, 264.

Appendix: calculation of the mean number of jumps of Ge atoms due to electron-beam stimulated migration

The exchange of a Ge atom and a monovacancy can occur if a Ge atom receives an enthalpy greater than the activation enthalpy h^{m}_{Ge}. This enthalpy can be obtained either via a thermally activated process or from energy it receives in a collision with a high-energy electron. The diffusion that occurs because of an atom receiving energy from the incident electron beam is denoted an electron-stimulated migration process [10, 11]. According to the model described in ref. 10, the jump frequency of a Ge atom that migrates in an Al matrix because of a 1 MeV electron irradiation is:

$$j = n\phi\sigma_m \tag{A1}$$

where ϕ is the flux of electrons passing through the specimen, n the concentration of monovacancies in the first nearest-neighbor shell of atoms surrounding a Ge atom, and σ_m the cross-section of a Ge atom receiving a kinetic recoil energy greater than h^{m}_{Ge}. The cross-section σ_m is an integral of a differential cross-section:

$$\sigma_m = \int_{h^{m}_{Ge}}^{T_m} d\sigma \tag{A2}$$

where T_m is the maximum recoil energy; for a 1 MeV electron irradiation $T_m = 60$ eV. Using the McKinley–Feshbach differential cross-section [24] we obtain:

$$\sigma_m = \pi\left(\frac{Ze^2}{mc^2}\right)^2\left(\frac{1}{\beta^4\gamma^2}\right)\left[\left(\frac{T_m}{h^{m}_{Ge}} - 1\right) - \beta^2 \ln\frac{T_m}{h^{m}_{Ge}} + \pi\alpha\beta\left\{2\left[\left(\frac{T_m}{h^{M}_{Ge}}\right)^{1/2} - 1\right] - \ln\frac{T_m}{h^{m}_{Ge}}\right\}\right] \tag{A3}$$

where

$$\gamma = 1 + \frac{E}{mc^2}, \qquad \beta^2 = 1 - \frac{1}{\gamma^2} \quad \text{and} \quad \alpha = \frac{Z}{137}$$

E is the kinetic energy of the incident electrons; e and m the charge and rest mass of an electron; c the speed of light and Z the atomic number of the recoiling atom. For $h^{m}_{Ge} = 0.64$ eV and $Z = 32$ we obtain the value $\sigma_m = 3.6 \times 10^{-21}$ cm^2.

The value of n depends on the monovacancy concentration under irradiation (c'_{lv}) and the coordination number of a Ge atom (z). If we take $c'_{lv} = 2.78 \times 10^{-3}$, the saturation concentration of electron irradition-induced vacancies in pure Al [43] and $z = 12$, then $n = zc'_{lv} = 0.033$; for $\phi = 3 \times 10^{19}$ cm^{-2} s^{-1} we obtain $j = 3.6 \times 10^{-3}$ s^{-1}. The root mean squared electron-beam stimulated diffusion distance of a Ge atom in Al is then:

$$\sqrt{x^2} = \frac{a_0}{\sqrt{2}}\sqrt{jt} \tag{A4}$$

where $a_0 = 0.405$ nm is the lattice constant of Al and t the irradiation time; for $t = 8333$ s, the time to accumulate Φ_c between 10 and 160 K, the value of $\sqrt{x^2} = 1.57$ nm. This value is 1.7 times the mean range of recoil-implanted Ge atoms (roughly 0.9 nm) and 7.9 times the straggling distance (0.2 nm) in Al. Note that the root mean squared electron-beam stimulated diffusion distance, given by eqn. (A4), is independent of temperature, *i.e.* it causes an athermal component to the diffusion process that must be added to the thermally activated component of diffusion to yield the net root mean squared diffusion distance of a Ge atom in Al.